■ 2622

# Underwater Image De-nosing using Discrete Wavelet Transform and Pre-whitening Filter

**Mohanad Najm Abdulwahed\*, Ali kamil Ahmed**
Materials Department, University of Technology, Baghdad, Iraq
\*Corresponding author, e-mail: mohanad.najm@yahoo.com

***Abstract***

*Image denoising and improvement are essential processes in many underwater applications. Various scientific studies, including marine science and territorial defence, require underwater exploration. When it occurs underwater, noise power spectral density is inconsistent within a certain range of frequency, and the noise autocorrelation function is not a delta function. Therefore, underwater noise is characterised as coloured noise. In this study, a novel image denoising technique is proposed using discrete wavelet transform with different basis functions and a whitening filter, which converts coloured noise characteristics to white noise prior to the denoising process. Results of the proposed method depend on the following performance measures: peak signal-to-noise ratio (PSNR) and mean squared error. The results of different wavelet bases, such as Debauchies, biorthogonal and symlet, indicate that the denoising process that uses a pre-whitening filter produces more prominent images and better PSNR values than other methods.*

*Keywords: underwater noise, denoising, wavelet transform, PSNR, whitening*

## 1. Introduction

Efficient underwater image denoising is a critical aspect for many applications [1]. Underwater images present two main problems: light scattering that alters light path direction and colour change. The basic processes in underwater light propagation are scattering and absorption. Underwater noise generally originates from man-made (e.g. shipping and machinery sounds) and natural (e.g. wind, seismic and rain) sources. Underwater noise reduces image quality [1, 2], and denoising has to be applied to improve it [3]. Underwater sound attenuation is dependent on frequency. Consequently, power spectral density $(PSD)$ for ambient noise is defined as coloured [4]. Many image denoising techniques are described in [5-9]. A method based on adaptive wavelet with adaptive threshold selection was suggested in [5] to overcome the underwater image denoising problem. Assume that an underwater image has a small signal-to-noise ratio (SNR) and image quality is poor. The simulation results show that the proposed method successfully eliminates noise, improves the peak SNR (PSNR) output of the image and produces a high-quality image. Light is repeatedly deflected and reflected by existing particles in the water due to the light scattering phenomenon, which degrades the visibility and contrast of underwater images. Therefore, underwater images exhibit poor quality. To process images further, wavelet transform and Weber's law were proposed in [8]. Firstly, several pre-processing methodologies were conducted prior to wavelet denoising thresholding. Then, Weber's law was used for image enhancement along with wavelet transform. Consequently, the recovered images were enhanced and the noise level was reduced. In the current study, a novel image denoising method is proposed in the presence of underwater noise using a pre-whitening filter and discrete wavelet transform (DWT) with single-level estimation.

## 2. Characteristics of Ambient Noise

The characteristics of underwater noise in seas have been discussed extensively [10]. Such noise has four components: turbulence, shipping, wind and thermal noises. Each component occupies a certain frequency band of spectrum. The PSD of each component is expressed as [11-13].

$$N_t(f) = 17 - \log f \tag{1}$$

$$N_s(f) = 40 + 20(s - 5) + 26 \log f - 60 \log(f + 0.03) \tag{2}$$

$$N_w(f) = 50 + 7.5 v_m^{\frac{1}{2}} + 20 \log f - 40 \log(f + 0.4) \tag{3}$$

$$N_{th}(f) = -15 + 20 \log f \tag{4}$$

where f represents the frequency in KHz. Therefore, the total PSD of underwater noise for a given frequency f (kHz) is

$$S_{xx}(f) = N_t(f) + N_s(f) + N_w(f) + N_{th}(f) \tag{5}$$

Figure 1 presents the experimental noise PSD in deep water under various activities conditions for shipping with a fixed speed of wind of (3.6 m/s). Each noise source is dominant in certain frequency bands, as indicated in Table 1.

Table 1. UWAN Band

| Band | Type |
| --- | --- |
| 0.1Hz - 10Hz | Turbulence noise |
| 10Hz - 200Hz | Shipping noise |
| 0.2 kHz - 100 kHz | Wind noise |
| above 100 kHz | Thermal noise |

## 3. Image Model

Noise interference is a common problem in digital communication and image processing. An underwater noise model for image denoising in an additive coloured noise channel is presented in this section. Numerous applications assume that a received image can be expressed as (6):

$$x(n) = s(n) + v(n) \tag{6}$$

where $s(n)$ is the original image and $v(n)$ denotes underwater noise. Hence, denoising aims to eliminate the corruption degree of $s(n)$ caused by $v(n)$. The power spectrum and autocorrelation of additive white Gaussian noise (AWGN) are expressed as (7, 8) [14]:

$$R_{vv}(m) = E\{v(m)v(m + k)\} = \sigma_v^2 \delta(m) \tag{7}$$

$$s_{vv}[e^{j2\pi f}] = DFT_{m \to f}\{R_{vv}(k)\} = \sigma_v^2 \qquad \frac{-f_s}{2} \leq f \leq \frac{f_s}{2} \tag{8}$$

The PSD of AWGN remains constant across the entire frequency range, in which all ranges of frequencies have a magnitude of $\sigma_v^2$. The probability distribution function $\rho_v(v)$ for AWGN is specified by [15]

$$\rho_v(v) = \frac{1}{\sigma_v \sqrt{2\pi}} e^{-\frac{v^2}{2\sigma_v^2}} \tag{9}$$

where $\sigma_v$ represents the standard deviation. With regard to autocorrelation functions, the delta function indicates that adjacent samples are independent. Therefore, observed samples are considered independent and identically distributed.

Underwater noise is dependent on frequency [16, 17]; hence, the assumption that it is AWGN is invalid, and instead, it is suitably modelled as coloured noise [1, 2, 18]. The PSD of coloured noise is defined as [19, 20]

$$S_{VV}(e^{j2\pi f}) = \frac{1}{f^\beta} \qquad \beta > 0, \qquad \frac{-f_s}{2} \le f \le \frac{f_s}{2} \tag{10}$$

However, the $R_{vv}[m]$ of coloured noise is not like a delta function, but, it is takes the formula of a $sinc(\ )$ function [14, 19]. In contrast to AWGN, noise samples are correlated [20].

## 4. Whitening Filter and Inverse Whitening Filter

A linear time-invariant whitening filter can be used to transform coloured noise into white noise [14, 21]. Through the transfer function $H(z)$, the prediction error filter (PEF) is used for whitening purposes [20, 22]. The output of PEF is determined as the difference between the actual and estimated sequences of the linear predictor. The one-step-forward predictor filter is expressed as

$$\dot{x}(n) = -\sum_{\lambda=1}^{p} a_p(\lambda)x(n-\lambda) \tag{11}$$

where p shows the length of the designed filter. $a_p(n)$ represents the coefficient of filter. The forward prediction error is defined as [20]

$$e_p(n) = x(n) - \dot{x}(n) = x(n) + \sum_{\lambda=1}^{p} a_p(\lambda)x(n-\lambda) \tag{12}$$

The filter coefficients can be estimated by minimising mean squared error (MSE). The transfer function of a filter can then be defined as

$$H_p(z) = \frac{E_p(z)}{X(z)} = 1 + a_1 z^{-1} + a_2 z^{-2} + \cdots + a_p z^{-p} \tag{13}$$

If the order of the PEF is suitably large, then the output of filter becomes white noise [20].

The output of PEF filter $x_w(n)$ denotes the process of convolution between a noisy image $x(n)$ and the impulse response of filter used in the whitening process $h_w(n)$. Therefore, the output of PEF is a coloured version of the original image in white noise.

$$x_w(n) = x(n) * h_w(n) = s(n) * h_w(n) + v(n) * h_w(n) \tag{14}$$

After the filter coefficients are determined, the noise term $v(n) * h_w(n)$ is minimised through a denoising process, thereby producing a clean version of the transformed image as follows:

$$\hat{s}_w(n) = s(n) * h_w(n) \tag{15}$$

An inverse whitening filter (IWF) can be used to recover the original image [23]. $h_{IWF}(n)$ denotes the impulse response of the IWF. The recovered image is

$$\hat{s}(n) = \hat{s}_w(n) * h_{IWF}(n) = s(n) * h_w(n) * h_{IWF}(n) \tag{16}$$

$H_{IWF}(z) = {}^1/_{H(z)}$ represents the relationship between the whitening and inverse whitening filters. The image recovered in the z-domain can be defined as

$$\hat{S}(z) = S(z).H_P(z).H_{IWF}(z) = S(z) \tag{17}$$

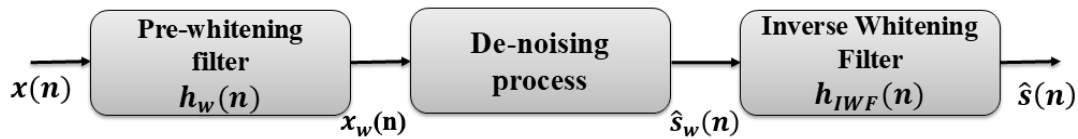The previously described overall process is illustrated in Figure 1.

Figure 1. Overall diagram of the denoising method that uses whitening and pre-whitening processes.

## 5. Image Denoising

Wavelets are used in image processing for sample edge detection, watermarking, compression, denoising and coding of interesting features for subsequent classification [24, 25]. The following subsections discuss image denoising by thresholding the DWT coefficients.

### 5.1. DWT of an Image Data

An image is presented as a 2D array of coefficients. Each coefficient represents the brightness degree at that point. Most herbal photographs exhibit smooth colouration variations with excellent details represented as sharp edges among easy versions. Clean variations in colouration can be strictly labelled as low-frequency versions, whereas pointy variations can be labelled as excessive-frequency versions. The low frequency components (i.e. smooth versions) establish the base of a photograph, whereas the excessive-frequency components (i.e. the edges that provide the details) are uploaded upon the low-frequency components to refine the image, thereby producing an in-depth image. Therefore, the easy versions are more important than the details. Numerous methods can be used to distinguish between easy variations and photograph information. One example of these methods is picture decomposition via DWT remodelling. The different decomposition levels of DWT are shown in Figure 2.
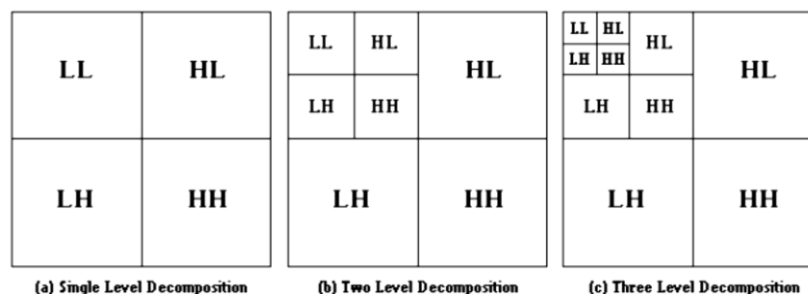


Figure 2. DWT decomposition levels

### 5.2. The Inverse DWT of an Image

Different classes of data are collected into a reconstructed image by using reverse wavelet transform. A pair of high- and low-pass filters is also used during the reconstruction process. This pair of filters is referred to as the synthesis filter pair. The filtering procedure is simply the opposite of transformation; that is, the procedure starts from the highest level. The filters are firstly applied column-wise and then row-wise level by level until the lowest level is reached.

## 6. Proposed Method

The following steps describe the image denoising procedure that uses a pre-whitening filter.

1) The pre-whitening process is performed on a noisy image using PEF to convert coloured noise to white noise.
2) The DWT of a noisy image is computed.
3) Noise variance is estimated by using the following robust median estimator:
4)

$$\sigma_v = \frac{median(|X_D(n,k)|)}{0.6745} \qquad (18)$$

where $X_D(n,k)$ represents all the coefficients of the wavelet detail in level k.

5) A soft threshold is applied to the sub-band coefficients for each sub-band, except for the low-pass or approximation sub-band.
6)

$$X_{D,\gamma}(n,k) = \begin{cases} sgn(X_D(n,k))(|X_D(n,k)| - \gamma_k) & if\ |X_D(n,k)| > \gamma_k \\ 0 & if\ |X_D(n,k)| \le \gamma_k \end{cases} \qquad (19)$$

where $\gamma_k$ denotes the threshold value in level k, and $X_{D,\gamma}(n,k)$ represents the wavelet detail coefficients after the thresholding process in level k.

7) The image is reconstructed by applying inverse DWT to obtain the denoised image. Figure 3 shows the data flow diagram of the image denoising process.
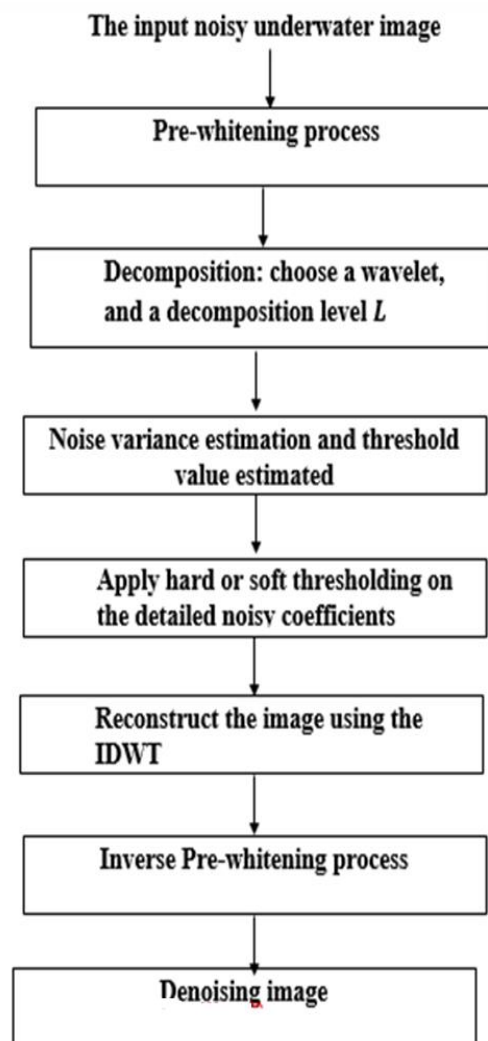


Figure. 3 Data flow diagram of image denoising using a pre-whitening filter.

### 6.1. Performance Measures

Common measurement parameters for image reliability include mean absolute error, normalized MSE (NMSE), PSNR and MSE [26]. An SNR over 40 dB provides excellent image quality that is close to that of the original image; an SNR of 30–40 dB typically produces good image quality with acceptable distortion; an SNR of 20–30 dB presents poor image quality an SNR below 20 dB generates an unacceptable image [27].

The calculation methods of PSNR and NMSE [28] are presented as follows:

$$\text{PSNR} = 10 \, log_{10} \frac{255^2}{MSE} \tag{20}$$

where MSE is the MSE between the original image ($x$) and the denoised image ($\hat{x}$) with size M×N:

$$\text{MSE} = \frac{1}{M * N} \sum_{i=1}^{M} \sum_{f=1}^{N} [x(i,j) - \varkappa(i,j)]^2 \tag{21}$$

### 7. Results and Discussion

MATLAB is used as the experimental tool for simulation, and simulation experiments are performed on a diver image to confirm the validity of the algorithm. The simulations are achieved at PSNR ranging from 30 dB to 60 dB by changing noise power from 0 dB to 15 dB. The applied order of the whitening filter is 10. Different denoising wavelet biases (i.e. Debauchies, biorthogonal 1.5 and symlet) are tested on an image with underwater noise via numerical simulation. As shown in Figure 4, soft thresholding and four decomposition levels are used.

Tables 2, 3 and 4 show the performance of the proposed method on various noise power based on the Debauchies, symlet and biorthogonal wavelet biases, respectively. The PSNR and MSE values are calculated based on each noise power value.

Table 2. Performance Results of PSNR and MSE on Diver Image Based on Debauchies Wavelet Bias

| Noise power (db) | PSNR | MSE |
| --- | --- | --- |
| 0 | 58.7275 | 0.0878 |
| 3 | 53.1670 | 0.3161 |
| 5 | 50.0854 | 0.6426 |
| 10 | 39.9653 | 6.6062 |
| 15 | 30.2530 | 61.8279 |

Table 3. Performance Results of PSNR and MSE on Diver Image Based on Symlet Wavelet Bias

| Noise power (db) | PSNR | MSE |
| --- | --- | --- |
| 0 | 58.8266 | 0.0859 |
| 3 | 53.3248 | 0.3048 |
| 5 | 50.0299 | 0.6509 |
| 10 | 40.0077 | 6.5420 |
| 15 | 30.0591 | 64.6499 |

Table 4. Performance Results of PSNR and MSE on Diver Image Based on Biorthogonal Wavelet Bias

| Noise power (db) | PSNR | MSE |
| --- | --- | --- |
| 0 | 58.7560 | 0.0873 |
| 3 | 53.4219 | 0.2981 |
| 5 | 50.2130 | 0.6240 |
| 10 | 39.7970 | 6.8672 |
| 15 | 30.0840 | 64.2804 |

| Biases type | Noisy image | De-noise image | PSNR (dB) |
|---|---|---|---|
| Sym3 | | | 50.02 dB |
| Sym3 | | | 30.05dB |
| *db*6 | | | 53.167 dB |
| *db*6 | | | 30.253 dB |
| Biorthogonal 1.5 | | | 53.421 dB |
| Biorthogonal 1.5 | | | 30.084 dB |

Figure. 4 Simulation results on diver image using different wavelet biases.

## 8. Conclusion

Underwater noise is mainly characterised as non-white and non-Gaussian noise. Therefore, traditional methods used for image denoising using wavelet transform underwater

are inefficient because these methods use only a single level for noise variance estimation and then apply it to other levels. However, noise variance at each level should be independently estimated in coloured noise. The traditional wavelet denoising method can be efficiently used with PSNR and MSE within an acceptable range by using a pre-whitening filter that converts underwater noise to white noise, as demonstrated by the results.

**Refrences:**
[1]  G Burrowes, J Y Khan, *Short-range underwater acoustic communication networks*: INTECH Open Access Publisher, 2011.
[2]  T Melodia, H Kulhandjian, L-C. Kuo, E Demirors. Advances in underwater acoustic networking. *Mobile Ad Hoc Networking: Cutting Edge Directions.* 2013: 804-852.
[3]  H Olkkonen. Discrete wavelet transforms: Algorithms and applications. *InTech, August,* 2011.
[4]  A Z. Sha'ameri, Y Y Al-Aboosi, N H H. Khamis. Underwater acoustic noise characteristics of shallow water in tropical seas. in *Computer and Communication Engineering (ICCCE), 2014 International Conference on,* 2014; 80-83.
[5]  M P A. Jaiswal, V. B. Padole. Implementation of an Improved Algorithm for Underwater Image Enhancement and Denoising.
[6]  L Fei, W. Yingying. *The research of underwater image de-noising method based on adaptive wavelet transform.* in Control and Decision Conference (2014 CCDC), The 26th Chinese, 2014: 2521-2525.
[7]  R Sathya, M Bharathi, G Dhivyasri. *Underwater image enhancement by dark channel prior.* in Electronics and Communication Systems (ICECS), 2015 2nd International Conference on, 2015: 1119-1123.
[8]  S Jian, W. Wen. *Study on Underwater Image Denoising Algorithm Based on Wavelet Transform.* in Journal of Physics: Conference Series, 2017: 012006.
[9]  R Schettini, S Corchs. Underwater image processing: state of the art of restoration and image enhancement methods. *EURASIP Journal on Advances in Signal Processing.* 2010: 746052.
[10]  R J Urick. Principles of underwater sound. 1983. ed: McGraw-Hill, 1983.
[11]  T Melodia, H Kulhandjian, L C Kuo, E. Demirors. Advances in Underwater Acoustic Networking. *Mobile Ad Hoc Networking: Cutting Edge Directions, Second Edition.* 2013*:* 804-852.
[12]  G Burrowes, J Y Khan. Short-Range Underwater Acoustic Communication Networks. *Autonomous Underwater Vehicles, Mr. Nuno Cruz (Ed.),* 2011.
[13]  Y Y Al-Aboosi, A Kanaa, A Z Sha'ameri, H A Abdualnabi. Diurnal Variability of Underwater Acoustic Noise Characteristics in Shallow Water. *TELKOMNIKA Telecommunication Computing Electronics and Control,* 2017; 15: 314, 2017.
[14]  A V Oppenheim, G C Verghese. Signals, systems, and inference. *Class notes for.* 2010: 6.
[15]  S M Kay. Fundamentals of statistical signal processing, Vol. II: Detection Theory. *Signal Processing. Upper Saddle River, NJ: Prentice Hall,* 1998.
[16]  R J Urick. Ambient noise in the sea. DTIC Document1984.
[17]  M Stojanovic, J. Preisig. Underwater acoustic communication channels: Propagation models and statistical characterization. *Communications Magazine, IEEE.* 2009; 47: 84-89, 2009.
[18]  M Chitre, J Potter, O S Heng. Underwater acoustic channel characterisation for medium-range shallow water communications. in *OCEANS'04. MTTS/IEEE TECHNO-OCEAN'04,* 2004: 40-45.
[19]  M L a W Zhao. Review Article On 1/f Noise. *Hindawi Publishing Corporation Mathematical Problems in Engineering.* 2012; 2012.
[20]  C W Therrien, *Discrete random signals and statistical signal processing*: Prentice Hall PTR, 1992.
[21]  J P C Da Costa, K Liu, H C So, S Schwarz, M Haardt, F Römer. Multidimensional prewhitening for enhanced signal reconstruction and parameter estimation in colored noise with Kronecker correlation structure. *Signal Processing,* 2013;. 93: 3209-3226.
[22]  K Ngo, T Van Waterschoot, M G. Christensen, M Moonen, S H. Jensen. Improved prediction error filters for adaptive feedback cancellation in hearing aids. *Signal Processing.* 2013; 93: 3062-3075.
[23]  B Widrow , E Walach. Adaptive Inverse Control A Signal Processing Approach. Reissue edn. ed: John Wiley & Sons, Inc, 2008.
[24]  M Misiti, Y Misiti, G Oppenheim, J-M Poggi. Wavelet toolbox. *The MathWorks Inc., Natick, MA.* 1996; 15: 21.
[25]  D Baleanu. Advances in wavelet theory and their applications in engineering. *Physics and Technology.* 2012*:* 353-371.
[26]  C Tan, A Sluzek, G S GL, T Jiang. Range gated imaging system for underwater robotic vehicle. in *OCEANS 2006-Asia Pacific.* 2007: 1-6.
[27]  C Tan, G Seet, A Sluzek, D He. A novel application of range-gated underwater laser imaging system (ULIS) in near-target turbid medium. *Optics and Lasers in Engineering.* 2005; 43: 995-1009.
[28]  J Ellinas, T Mandadelis, A Tzortzis, L Aslanoglou. Image de-noising using wavelets. *TEI of Piraeus Applied Research Review.* 2004; 9: 97-109.